KnowEx Social Sciences
Vol.4, No.1, 65-105, 2026, ISSN 2705-9901 (Online)

DOI: https://doi.org/10.17501/27059901.2026.4104

A MULTI-INDEX APPROACH IN KURUNEGALA TO ASSESS URBAN GROWTH AND ENVIRONMENTAL TRANSFORMATIONS (1995-2024)

Kumari LGAS* and Liyanage DLNP

Department of Geography & Environmental Management, Faculty of Social Sciences & Languages, Sabaragamuwa University of Sri Lanka

Abstract: Urban expansion has become one of the most significant drivers of land use and environmental transformation in rapidly developing urban areas. This study develops a Landsat time series–based multi-index environmental assessment framework to examine the spatiotemporal dynamics of urban growth and associated environmental impacts in the Kurunegala Municipal Council area, Sri Lanka, from 1995 to 2024. Multi-temporal Landsat 5, 7, and 8 satellite imagery, along with census data, were analyzed using GIS and RS techniques. Land Use/Land Cover changes were first classified to quantify urban expansion, vegetation loss, and agricultural land transformation. Subsequently, vegetation dynamics were assessed using the NDVI, while urban growth patterns were evaluated using the NDBI. Thermal environmental changes were examined through LST and UHI analysis. An integrated ECI was developed by combining NDVI, NDBI, and LST to identify spatial environmental risk zones. The results indicate a substantial increase in built-up land by 31.9%, accompanied by a decline in dense vegetation cover and a reduction in agricultural land from 55% to 26.71%. LST increased significantly, reaching up to 34.1°C, with pronounced thermal hotspots concentrated in urban core areas. Correlation and regression analyses revealed a statistically significant negative relationship between NDVI and LST ($r < 0$, $p < 0.05$) and a positive relationship between NDBI and LST ($r > 0$, $p < 0.05$), confirming strong land–atmosphere interactions driven by urban expansion. The integrated ECI map identified approximately 27.4% of the study area as high environmental critical zones, highlighting areas vulnerable to thermal stress and ecological degradation. The findings demonstrate that rapid urban expansion, declining vegetation cover, and increasing surface temperatures are strongly interconnected processes shaping the urban environment of Kurunegala. This study provides a replicable GIS–RS-based analytical framework for monitoring urban environmental change and supporting sustainable urban planning and policy decision-making.

Keywords: *environment change, Kurunegala, Land Use and Land Cover, urban expansion*

Introduction

Global Context of Urbanization

Urban growth plays a significant role in improving access to housing, healthcare, education and transportation (Glaeser.,2011). According to the United Nations (2018), more than 55% of the global

*Corresponding author's email:*ajinisagarika1999@gmail.com*

population lives in urban areas and this figure is projected to reach 68% by 2050. Urban growth often leads to significant environmental changes, including deforestation, loss of green spaces, air pollution, and rising surface temperatures. Urban growth contributes significantly to global warming by altering land surfaces, increasing greenhouse gas (GHG) emissions, and intensifying the urban heat island (UHI) effect (IPCC, 2021). Urban areas experience higher temperatures than surrounding rural areas due to concrete, asphalt, and other heat-absorbing materials (Oke., 1982). Cities account for more than 70% of global CO2 emissions and consume more than two-thirds of the world's energy (UN-Habitat, 2020). The UHI effect, in which urban areas experience higher temperatures than surrounding rural areas due to the absorption of heat by concrete surfaces, further exacerbates global warming. Heat waves have intensified in major cities such as New York, Tokyo, and Beijing (Rosenzweig et al., 2018).

Study Area Background

The Kurunegala Municipal Council area has experienced significant urban growth since the late 20th century. According to Fernando (2018) Kurunegala urban growth is characterized by increased building, expansion of commercial zones and development of infrastructure, which in turn leads to significant land use changes. This growth often leads to significant environmental changes, including deforestation, loss of green spaces, air pollution and rising surface temperatures. The built-up area of Kurunegala grew by approximately 35% between 2000 and 2020, and the natural landscape was replaced by concrete structures (Perera et.al 2016). Urban growth within the municipal council area has changed the landscape, and satellite imagery analysis shows that forest cover in Kurunegala has decreased by about 20% from 1995 to 2024 due to land conversion for housing, commercial buildings, and road networks (Perera, M. 2016). A study by the Central Environmental Authority (2022) revealed that pollution levels in Kurunegala Lake have increased by 30% in the past decade. In addition, the urban heat island effect is more pronounced, with the city becoming warmer than its surrounding rural areas, with an increase in temperature of approximately 1.5C^0 over the past 25 years. (Fernando et al, 2018). Despite the potential of remote sensing, the lack of application of these techniques to assess the environmental impact of urban growth in Kurunegala is a problem. Based on the implications, a thorough analysis of its environmental implications is needed. Understanding the environmental impact of urban growth in Kurunegala using advanced RS techniques requires analysis using satellite imagery over decades.

Research Gap, Objectives and Significance of the Study

This paper presents an innovative approach using remote sensing technology to analyze the specific environmental consequences of urban growth in Kurunegala city. The study by Rajapaksa and Perera (2019) used a combination of remote sensing techniques, geographic information system (GIS) tools, and statistical methods to assess changes in land use patterns in Kurunegala city between 2000 and 2020. The secondary method for data collection was the use of remote sensing. Satellite images from two different time periods, 2000 and 2020, were obtained from Landsat satellite sources. GIS data was incorporated into the study to analyze land use patterns. In the data analysis, the researchers used maximum likelihood classification to classify the satellite images into different land use classes. A change detection analysis was performed to assess how land use has evolved over a 20-year period. In the study conducted by Nilantha et al. (2020), researchers aimed to assess the urban heat island (UHI) effect in Kurunegala city and used Landsat satellite imagery to collect data on land surface temperature (LST). To ensure the accuracy of temperature measurements obtained from satellite imagery, the researchers used the Thermal Infrared Band of Landsat imagery. The researchers performed a spatial analysis using GIS tools to map temperature variations across the study area.

The objectives of this research are to study the environmental impact of urban growth during the period 1995 to 2024 using remote sensing techniques and to examine the correlation between the environmental impacts of urban growth in the municipal council area. This research contributes empirical evidence. The significance of this research is the utilization of advanced remote sensing and GIS techniques for the study of existing urban growth. Satellite imagery, spatial analysis, and statistical modeling ensure a comprehensive assessment of urban growth dynamics. In addition, the study demonstrates how remote sensing can be used more cost-effectively than traditional field-based methods, allowing for large-scale and long-term monitoring of urban environments.

Materials and Methods

Study area

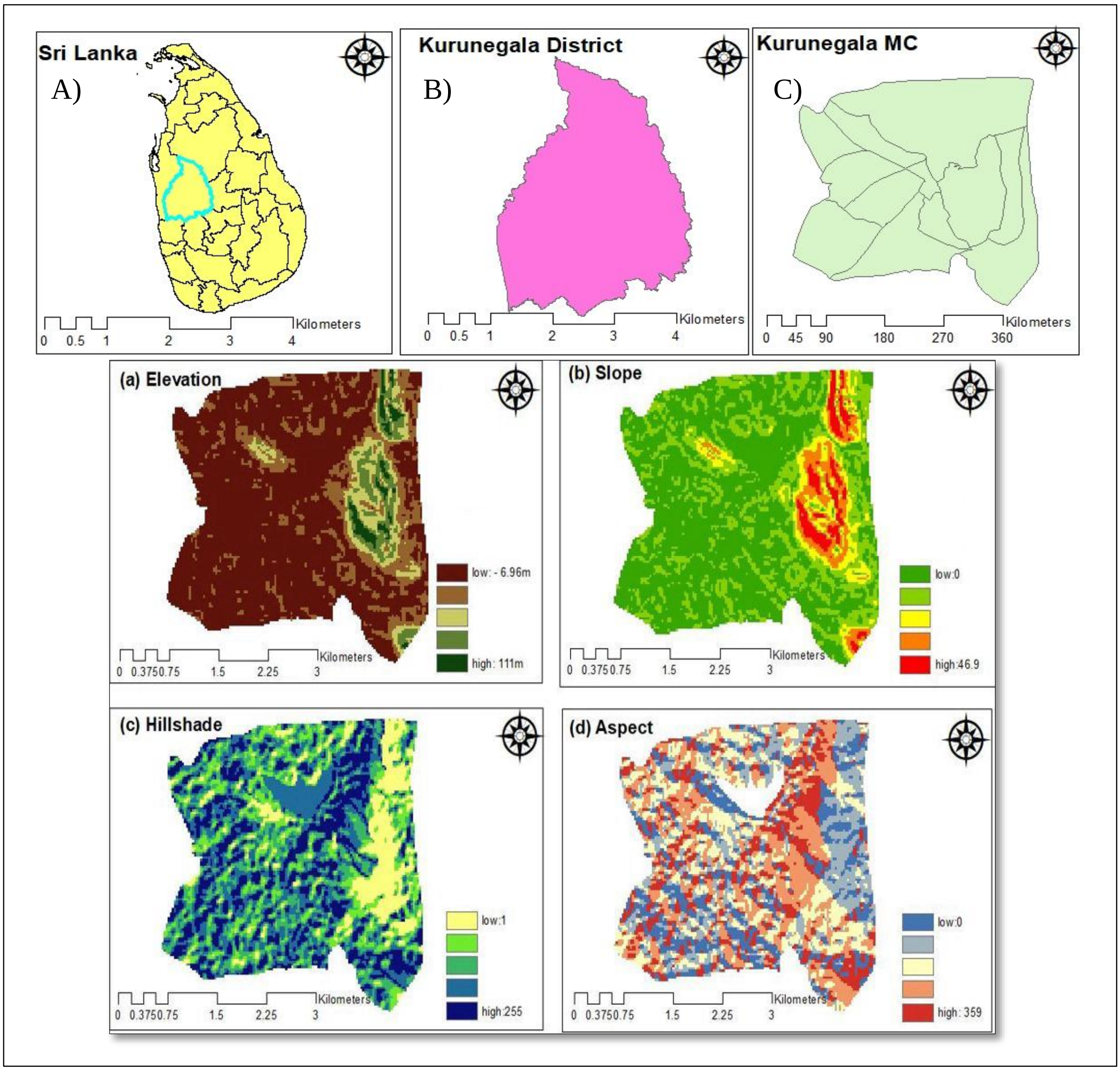

Figure1: A) Sri Lanka B) Kurunegala district C) Kurunegala MC

a) Elevation b) Slope c) Hillshade d) Aspect

Source: Created by author based on 1:50000 Survey Department data, 2025

The study area was conducted in the Kurunegala Municipal Council, Sri Lanka, located approximately between 7°28′–7°35′ N latitude and 80°20′–80°27′ E longitude. The area covers an extent of approximately 11.34 km² and represents a rapidly urbanizing regional urban center in the North Western Province. The region is characterized by a tropical monsoon climate, with high annual temperatures and distinct wet and dry seasons. The terrain consists of undulating topography with scattered hills and low-lying plains, influenced by surrounding natural features such as Kurunegala Lake and agricultural landscapes. Kurunegala has experienced rapid urban expansion driven by administrative importance, transportation connectivity, and commercial development, making it a suitable case study for analyzing long-term urban environmental change. The study area was selected due to: rapid land conversion from vegetation/agriculture to built-up land, observed urban heat island intensification, availability of long-term satellite data coverage and also its importance as a regional growth center.

Materials used

This research was based on secondary data. The main source of secondary data used was satellite imagery. It was collected from the USGS Earth Explorer website. As institutional data, demographic data of the Kurunegala Municipal Council area and a description of the study area were obtained from the Municipal Council, while land use data within the area was also collected from the Kurunegala Urban Development Authority.

Table 1: Satellite data description

Sensor type	Date	Path/Row	Spatial Resolution	Season	Cloud cover%
Landsat 5 TM	1995.04.07	141/055	30 m	Dry/Wet	<30%
Landsat 5 TM	200507.07	141/055	30 m	Dry/Wet	<30%
Landsat7 ETM+	2015.04.14	141/055	30 m	Dry/Wet	<30%
Landsat 8 OLI/TIRS	2024.07.03	141/055	30 m	Dry/Wet	<30%

Source: USGS, 2025

Methods used

The study uses a combination of established remote sensing techniques (NDVI, NDBI, LST) and statistical analysis to examine urban growth and its environmental impact. The scientific rationale behind this study is that a comprehensive understanding of urban growth and environmental impacts in forested areas that are experiencing rapid urban growth is needed Several key steps were taken to create LULC maps and RS indices, including image preprocessing, classification, accuracy assessment, calculation of RS indices and statistical analysis to analyze the statistical correlations between environmental impacts.

A broad technical flow chart depicting the research process that includes these stages is shown in Figure 2 below.

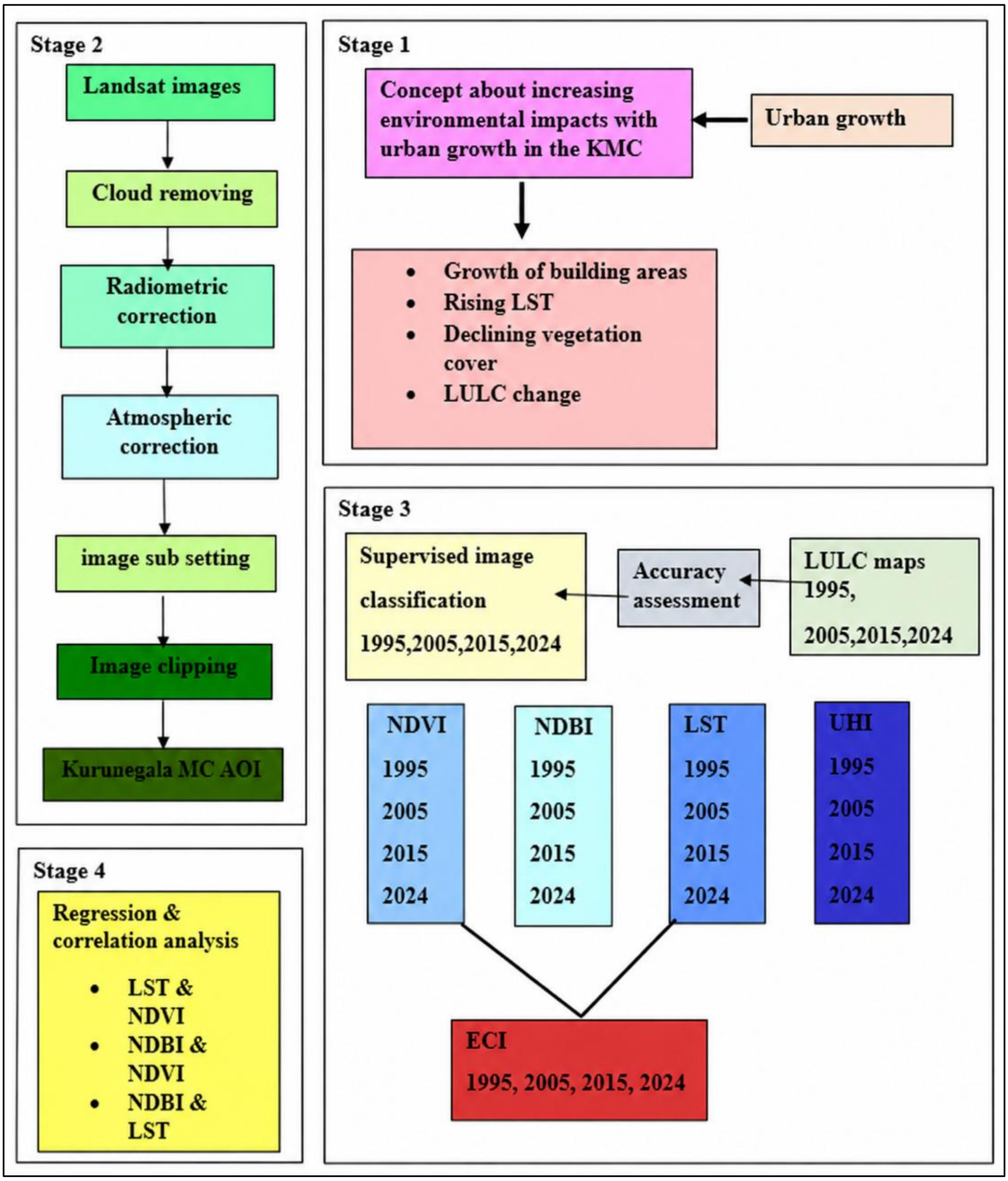

Figure 2: Methodological flowchart of the study, 2025

Source: Created by author,2025

Image Processing

The USGS radio-metrically calibrated and atmospherically corrected Landsat collection 2 Level-1 was used.

Satellite images with low cloud cover (less than 30%) were downloaded when downloading Landsat images. These Landsat images were used to calculate NDVI, NDBI, LST, for the analysis of the environmental impact of urban growth in the Kurunegala Municipal Council area during the years 1995, 2005, 2015, and 2024. To ensure radiometric consistency across time series, Top of Atmosphere (TOA) reflectance conversion and atmospheric correction were applied using standard Landsat calibration coefficients (USGS, 2023). Cloud-contaminated pixels (>30%) were excluded using QA bands.

Image Classification

Landsat images were used to determine the LULC (Land Cover/Land Use) change that has occurred with urban growth, and Landsat 5 TM and Landsat 8 OLI/TIRS satellite images were downloaded from USGS Earth Explorer for the years 1995, 2005, 2015, and 2024 as shown in Table 3. 6. Arc GIS 10.4, and ERDAS Imagine 2011 were used in various stages of the analysis. All images have the same spatial resolution of 30m. The study area was integrated into the satellite image using the Extract by mask tool using the 2,3,4,5,6,7 bands composite band tool for the years 1995, 2015, 2015 and 2024 using Arc GIS 10.4 software. This combination typically shows urban areas as blue, vegetation as red, water bodies as dark blue to black, and bare and bare land as white. The Maximum Likelihood Classification (MLC) method was used to analyze Landsat images to create LULC maps for the relevant years. This classification was done in three steps from Step 1 to Step 3.

> Step 1 - Preparation of Land Use/Land Cover (LULC) classes (Through this, each land use was identified and classes were created for them. Here, 5 land use types have been identified for this research.
>
> Step 2 - Extraction of signatures (This is done after providing the samples and in this step, a signature (gsg) file was created for each information class. These files contain various information about the described land use classes.)
>
> Step 3 - Supervised Classification (The next step is to classify the images based on these signature (gsg) files.)

Details of the land use classes with the relevant codes are shown in Table 2 below.

Table 2: Details of land use classes with relevant codes, 2025

Refs.	LU/LC	Details
BA	Buildup area	Areas with buildings, roads, man-made structures. Residential, commercial, and industrial zones
VG	Vegetation	Natural or semi-natural plant cover, including forests, shrubs, and grasslands.
WB	Waterbody	Rivers, lakes, ponds, tanks
AL	Agriculture land	Seasonal or perennial crops, plantations
BL	Bare land	Rocky terrain, areas without vegetation

Source: Created by author, 2025

Accuracy Assessment

In the accuracy assessment for land use classification, classification accuracy is measured by comparing two datasets. The standard way to do this is to create a confusion matrix using ground truth data. Here, for each year, the overall accuracy, user accuracy, producer accuracy, and kappa coefficient were calculated. The overall accuracy is presented as a percentage with 100% accuracy. Individual classes were calculated using the user accuracy and producer accuracy. Producer accuracy represents how often the points on the classified map are correctly located on the correct ground. Producer accuracy represents how often the points on the map are correctly located on the ground.

Accuracy Metrics

- Overall Accuracy (OA) (Congalton,1991)
- Producer's Accuracy (PA)
- User's Accuracy (UA)
- Kappa Coefficient (κ) (Cohen, 1960)

Kappa Formula

$$K = \frac{Po - Pe}{1 - Pe}$$

Where:

- P_o = observed agreement
- P_e = expected agreement by chance

Spectral Indices

NDVI - Vegetation Assessment

NDVI was used in this study to assess surface vegetation cover and determine vegetation presence at specific locations. NDVI values range from −1 to 1, with negative values typically indicating water bodies (saputra et al.,2013) The following equation was used to calculate NDVI. Where the NIR band represents Band 4 (0.76–0.90 µm) of Landsat TM and Band 5 (0.85–0.88 µm) of Landsat OLI, and the RED band represents Band 3 (0.63–0.69 µm) of Landsat TM and Band 4 (0.64–0.67 µm) of Landsat OLI (santos et al., 2017. estoque et al., 2017). NDVI values were classified into five land cover classes based on standard threshold ranges. Non-vegetation was defined as NDVI values less than 0.1. Low vegetation density ranged from 0.1 to 0.2, moderate vegetation from 0.2 to 0.4, high vegetation from 0.4 to 0.6, and very high vegetation density from 0.6 to 1.0. This classification scheme was used to distinguish vegetation health and density variations across the study period.

$$NDVI = (NIR - RED)/(NIR + RED)$$

NDBI - Built-up detection

The Normalized Difference Built-up Index (NDBI) was employed to detect and quantify built-up land expansion within the Kurunegala Municipal Council area from 1995 to 2024. NDBI was calculated using the Near Infrared (NIR) and Shortwave Infrared (SWIR) bands of Landsat imagery. For Landsat 5 TM, bands 4 and 5 were used, while Landsat 8 OLI bands 5 and 6 were utilized. The index was derived using Equation X, where positive values represent built-up surfaces and negative values indicate vegetation and water bodies. The generated NDBI maps were classified and analyzed to evaluate spatial patterns of urban expansion and impervious surface growth over time. The NDBI technique has been widely applied in urban studies due to its effectiveness in identifying built-up areas and monitoring urbanization processes (Zha et al., 2003; Xu, 2008; Chen et al., 2014). The MIR band represents Band 5 (1.55–1.75 µm) of Landsat TM and Band 6 (1.57–1.65 µm) of Landsat OLI, while the NIR band represents Band 4 (0.76–0.90 µm) of Landsat TM and Band 5 (0.85–0.88 µm) of Landsat OLI (Ranagalage et al., 2018; Tian et al., 2022).

$$NDBI = (MIR - NIR)/(MIR + NIR)$$

LST - Land Surface Temperature

Land Surface Temperature (LST) was derived to assess the spatial and temporal thermal characteristics of the Kurunegala Municipal Council area between 1995 and 2024. Landsat 5 Thematic Mapper (TM) imagery for 1995 and 2005 and Landsat 8 Operational Land Imager (OLI) and Thermal Infrared Sensor (TIRS) imagery for 2015 and 2024 were utilized. Thermal band 6 of Landsat 5 and thermal bands 10 and 11 of Landsat 8 were employed to retrieve surface temperature using the Radiative Transfer Equation (RTE) and Split-Window approaches. Digital Number (DN) values were converted into spectral radiance and subsequently transformed into brightness temperature. Land surface emissivity values were estimated using NDVI-based methods before calculating LST. The resulting temperature values were expressed in degrees Celsius and analyzed to identify thermal variations associated with urban growth and land-use changes (Weng et al., 2004; Sobrino et al., 2004; Avdan & Jovanovska, 2016). Here, five step from step 1 to step 4 were followed to calculate the land surface temperature.

Step 1- Calculated under generalized NDVI

$$NDVI = (NIR - RED) \,/\, (NIR + RED)$$

Step 2- Calculating the proportion of vegetation (PV)

$$PV = \left(\frac{NDVI - NDVI_{min}}{NDVI_{max} - NDVI_{min}}\right)2$$

Step 3 - Calculating land surface emissivity (LSE)

n=0.986 m=0.004

step 4 - Processing the emitted LSE values using equations

$$\frac{B}{1} + (\lambda * \frac{TB}{\varrho})\ ln\ \mathcal{E}$$

TB=thermal band

λ =10.8 for Landsat TIBS Band 10

ϱ =Boltzmann constant (14380)

Ɛ =land surface emissivity

UHI – Urban Heat Island calculation

Urban Heat Island (UHI) intensity was assessed to examine the thermal differences between urban and non-urban areas within the Kurunegala Municipal Council area. UHI intensity was calculated by comparing the mean Land Surface Temperature of built-up areas with the mean temperature of surrounding rural and vegetated areas. The spatial distribution of UHI was mapped using LST outputs derived from Landsat imagery for 1995, 2005, 2015, and 2024. Areas exhibiting higher temperatures than the surrounding environment were classified as urban heat islands. The analysis enabled the identification of temporal changes in thermal hotspots and their relationship with urban expansion and vegetation decline. Previous studies have demonstrated that increasing built-up surfaces and decreasing vegetation cover contribute significantly to UHI formation and intensification (Oke, 1982; Voogt & Oke, 2003; Rizwan et al., 2008).

$$UHI = LST_{max} - LST_{min}$$

ECI - Environmental Condition Index

The Environmental Criticality Index (ECI) was developed to evaluate the spatial distribution of environmental stress and ecological vulnerability within the Kurunegala Municipal Council area. The index was generated by integrating multiple environmental indicators, including Land Surface Temperature (LST), Normalized Difference Vegetation Index (NDVI), Normalized Difference Built-up Index (NDBI), and Normalized Difference Water Index (NDWI), within a GIS environment. Each indicator was standardized and assigned weights based on its relative contribution to environmental degradation. A weighted overlay analysis was then performed to produce the ECI map. The resulting index values were classified into non-critical, low-critical, moderate-critical, high-critical, and very high-critical categories to assess environmental conditions and identify areas experiencing greater ecological stress due to urbanization. Similar multi-criteria environmental assessment approaches have been widely used to evaluate environmental vulnerability and urban ecological conditions (Malczewski, 2006; Eastman, 2012; Geneletti, 2004).

$$ECI = \frac{LST(streched\ 1 - 255)}{NDVI(streched\ 1 - 255)}$$

Statically Analysis

The correlation between the previously calculated NDVI, NDBI, and LST indices is analyzed. The correlation was studied by keeping LST as the independent variable and NDVI as the dependent variable, and sometimes the correlation was studied by using NDBI as the independent variable and NDVI as the dependent variable, and NDBI as the independent variable and LST as the dependent variable.

Results and Discussion

Land Use/Land Cover Change Analysis

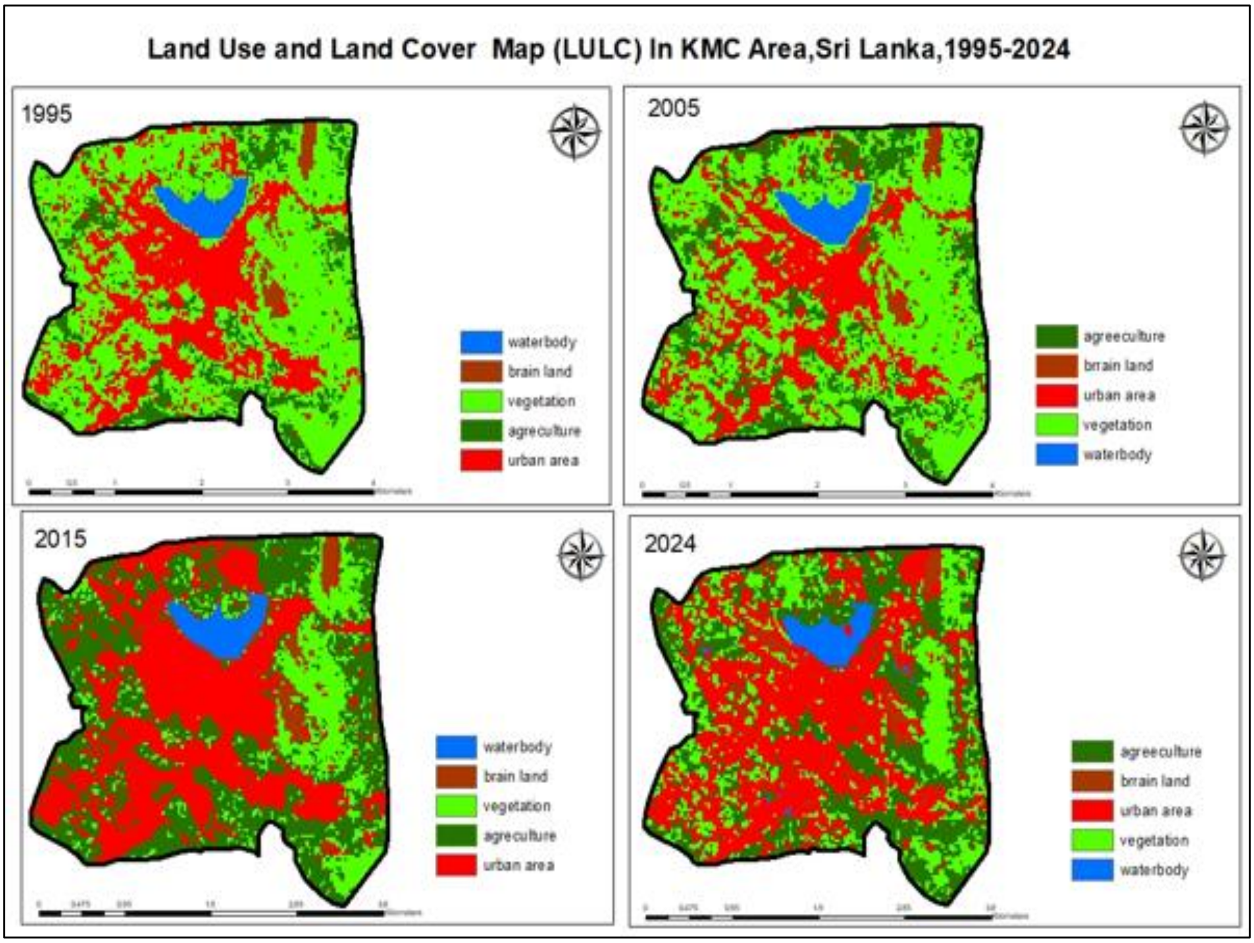

Figure 3: Land Use/Land Cover Map, Kurunegala Municipal Council Area, 1995-2024

Source: Created by the author based on 1:50000 maps of the Survey Department, 2025

The spatial distribution of LULC changes between 1995 and 2024 is presented in Figure 3 which demonstrates a clear transformation of the Kurunegala Municipal Council area from a predominantly vegetated landscape into an increasingly urbanized environment. The vegetation-covered area declined from 6.444 km² (55%) in 1995 to 3.149 km² (26.71%) in 2024, representing a substantial reduction of natural vegetation during the study period. In contrast, built-up areas increased from 2.91 km² (25%) in 1995 to 5.738 km² (48.67%) in 2024, indicating an expansion of approximately 97.2%.

This represents the dominant land transformation process within the study area. The increasing built-up surface indicates progressive conversion of vegetated and agricultural land into impervious surfaces associated with residential development, commercial activities, and infrastructure expansion. The increase in impervious surfaces has important environmental implications because such surfaces reduce evapotranspiration, increase heat absorption, and contribute to surface temperature increases. Agricultural land showed temporal variation, increasing from 1.429 km² (12%) in 1995 to 2.567 km²

(21.77%) in 2015 before declining to 2.216 km² (19%) in 2024. This temporary increase may reflect land-use transition processes before conversion into urban functions. The observed pattern agrees with previous studies that identify urban expansion as a major driver of vegetation loss and land surface modification in Sri Lankan cities (Rajapaksha & Perera, 2019). Similar urban land transformations have been reported in rapidly developing secondary cities where residential and infrastructure development replace natural land covers.

Table 3: LULC classification and their respective area, Kurunegala Municipal Council area, 1995-2024

Land Use Classes	1995		2005		2015		2024	
	km	%	km	%	km	%	km	%
Water body	0.35	3.14	0.36	3	0.375	3.18	0.37	3.3
Bare land	0.26	2	0.21	2	0.21	2	0.25	2.2
Agriculture	1.42	12	1.83	15.59	2.56	21.77	2.21	19
Vegetation	6.44	55	6.08	52	4.55	38.65	3.14	26.71
Buildup area	2.91	25	3.30	28	4.57	38.79	5.73	48.67

Source Created by the author based on the land environment/land map, 2025

Vegetation Dynamics Based on NDVI Analysis

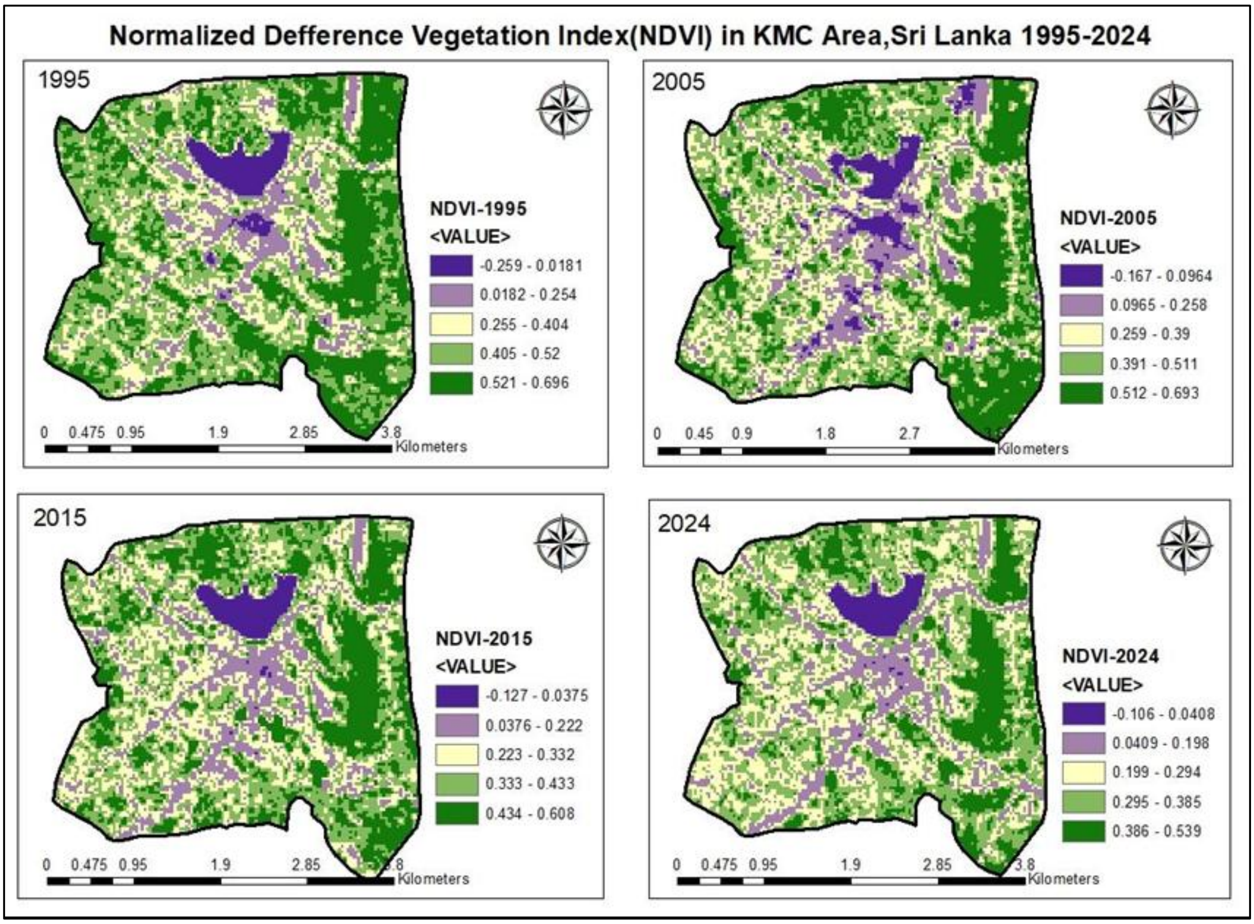

Figure 4: Normalized Change Vegetation Index, Kurunegala Municipal Council Area, 1995-2024

Source: Created by the author using Landsat data (1995–2024) from USGS Earth Explorer and the 1:50,000 topographic map from the Survey Department of Sri Lanka, 2025

NDVI analysis was conducted to evaluate changes in vegetation cover in the Kurunegala Municipal Council area from 1995 to 2024. By comparing NDVI values across different time periods, the study identified the extent and spatial pattern of vegetation change associated with urban expansion and land-use transformation. As shown in Figure 4, very high-density vegetation declined substantially from 34.95 km² (29.62%) in 1995 to 22.43 km² (19.01%) in 2024, indicating a significant reduction in dense natural vegetation. In contrast, moderate-density vegetation increased from 24.11 km² (20.44%) to 36.32 km² (30.78%), while non-vegetated areas expanded from 3.77 km² (3.20%) to 7.37 km² (6.25%).

Spatially, the most pronounced vegetation loss occurred in and around the Kurunegala urban core, particularly within the Kurunegala town center and its surrounding GN divisions, where rapid built-up expansion has replaced previously vegetated land. Noticeable reduction in high-density vegetation is also observed in the Ethugala forest fringe areas, indicating gradual encroachment and fragmentation of natural vegetation. Furthermore, areas surrounding Kurunegala Lake show clear changes, where portions of vegetated buffer zones have been converted into moderately vegetated and non-vegetated land uses due to infrastructure development and recreational activities.

These changes indicate a gradual conversion of dense vegetation into moderately vegetated and non-vegetated land uses, reflecting the environmental impacts of urban growth in the study area. The increase in non-vegetated areas reflects the expansion of built-up surfaces such as buildings, roads, and commercial zones, replacing natural land cover. Low-density vegetation shows a fluctuating trend over the study period, representing transitional land-use conditions where vegetation was partially degraded or converted. Overall, very high-density vegetation, which represents relatively undisturbed natural forest cover, recorded a continuous decline of 12.52 km² (35.8%) between 1995 and 2024. These findings are consistent with previous studies which report that rapid urban expansion typically leads to significant reductions in vegetation cover, fragmentation of forested areas, and increases in built-up land due to land-use conversion processes (Lambin & Geist, 2006; Seto et al., 2012; Herold et al., 2005). Overall, the results demonstrate a consistent reduction in dense vegetation cover corresponding with increasing urban expansion in the Kurunegala Municipal Council area.

Table 4: Area of Different NDVI Classes (km^2), Kurunegala Municipal Council, 1995 - 2024

	1995		2005		2015		2024	
NDVI classes	km	%	km	%	km	%	km	%
Non vegetation	3.77	3.2	3.83	3.25	4.77	4.04	7.37	6.25
Less density	12.33	10.46	18.34	15.55	16.20	13.74	16.39	13.9
Moderate density	24.11	20.44	29.56	25.06	32.43	27.49	36.31	30.78
High density	41.80	35.44	34.92	29.6	36.70	31.11	39.06	33.11
Very High density	34.94	29.62	27.77	23.54	28.8	24.41	22.42	19.01

Source: Created by the author based on the Normalized Difference Vegetation Index, 2025/

Built-up Expansion Dynamics Based on NDBI Analysis

NDBI analysis was undertaken to quantify the spatial and temporal dynamics of built-up surface expansion within the Kurunegala Municipal Council (KMC) area between 1995 and 2024. In 1995, NDBI values were predominantly low and negative across most parts of the study area, reflecting limited urban intensity and dominance of natural land surfaces. By 2024, the NDBI distribution shows a marked increase in positive values, confirming intensified urban expansion and higher concentrations of built-up surfaces. This increasing trend in mean NDBI values, along with shifts in minimum and maximum values over time (Figure 5), indicates growing urban heterogeneity and spatial expansion of impervious land cover.

This pattern is consistent with findings from previous studies, which have shown that NDBI is an effective indicator for monitoring urban expansion and built-up density changes over time (Zha et al., 2003; Yang et al., 2014). Similar research in South Asian urban environments has also reported that increasing NDBI values strongly correspond with rapid urban growth and conversion of vegetated land into built-up surfaces (Rimal et al., 2018; Dewan & Yamaguchi, 2009).

The land cover comparison further shows that built-up area increased from 2.91 km² in 1995 to 5.738 km² in 2024, representing a total increase of 2.828 km². This confirms a sustained and continuous expansion of urban land within the KMC boundary, particularly concentrated around the urban core and along major transportation corridors. However, this spatial expansion should be interpreted as a secondary validation of the spectral NDBI trends rather than the primary analytical output.

The observed increase in NDBI is also closely linked with broader environmental changes. Previous studies have established that rising NDBI values are typically associated with declining NDVI (vegetation loss) and increasing land surface temperature (LST), which collectively contribute to the formation and intensification of urban heat island (UHI) effects (Weng, 2001; Li et al., 2012). In rapidly urbanizing cities, the conversion of vegetated surfaces into impervious built-up land reduces evapotranspiration and increases heat absorption, thereby intensifying surface warming. Similar processes are likely occurring in Kurunegala, where increasing NDBI values suggest concurrent vegetation reduction and potential increases in thermal stress.

Overall, while localized urban development patterns such as expansion along major roads and established urban centers are visible, these serve only as supporting spatial evidence. The NDBI results provide the primary quantitative confirmation of urban expansion, and the observed trends are consistent with established literature on urban growth dynamics, vegetation decline, and urban climate change interactions.

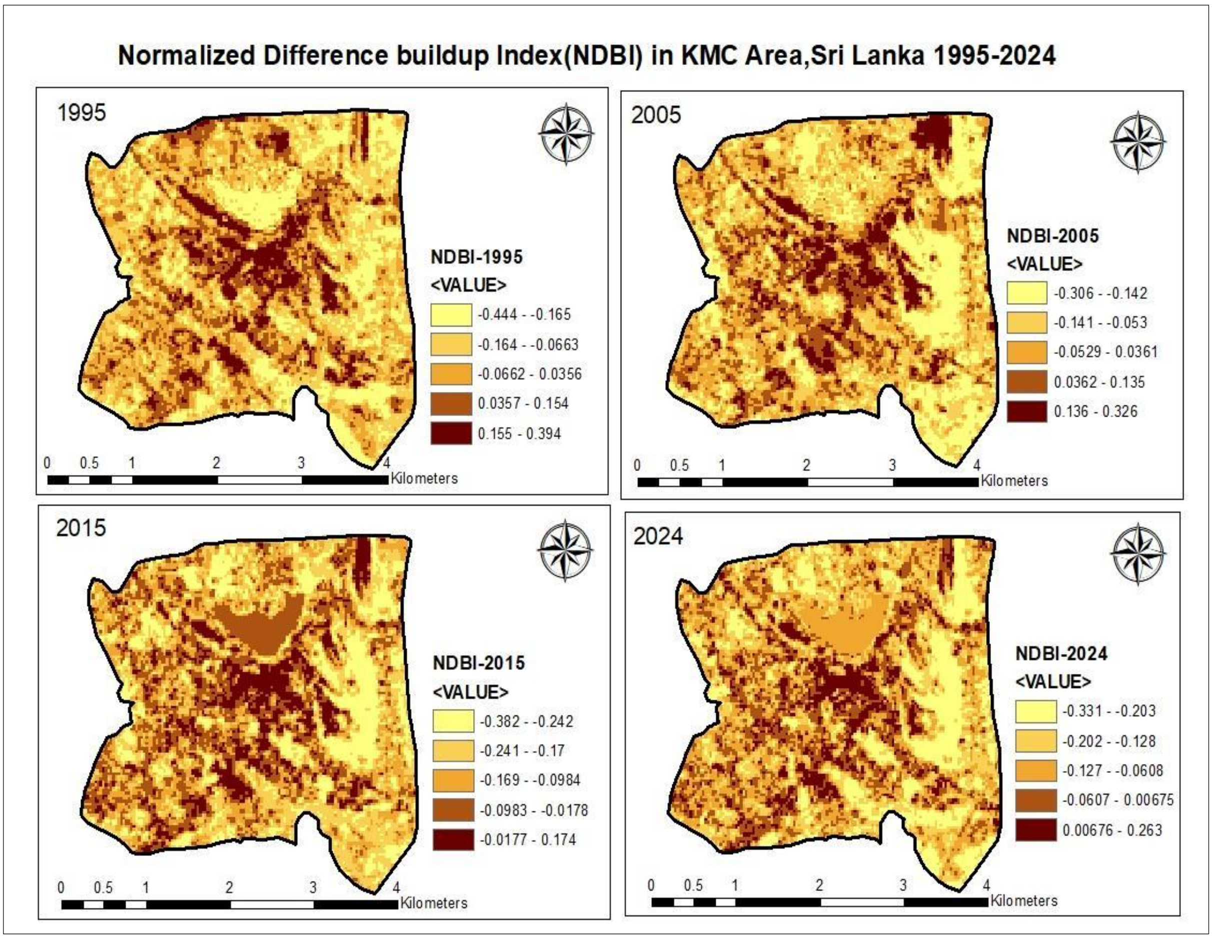

Figure 5: Normalized Difference Built Index (NDBI), Kurunegala Municipal Council Area, 1995 – 2024

Source: Created by the author using Landsat data (1995–2024) from USGS Earth Explorer and the 1:50,000 topographic map from the Survey Department of Sri Lanka, 2025

As urban built-up areas expand, people have access to the city's services. The increasing demographic pressure, including permanent and temporary population, has expanded the residential and commercial land cover. The central area of Kurunegala city is the nucleus of the city's urban fabric. In 1995, this area was characterized by medium-density residential units, administrative buildings and a moderate commercial footprint. By around 2005, the built-up character intensified with the expansion of the Kurunegala Teaching Hospital and the construction of modern government buildings such as the new Municipal Council Complex and regional office branches of state-owned banks such as the People's Bank and the Bank of Ceylon. By 2015, rapid vertical expansion had occurred and many older buildings had been replaced. By 2023, 2024, Kurunegala city, the central area, would exhibit characteristics of a high-density urban core. Due to space constraints, urbanization has expanded vertically and multi-story buildings have been constructed. Remote sensing and GIS analysis during this period show a significant increase in building index values across these zones. The shift from vegetated land cover to concrete surfaces is evident.

Land Surface Temperature (LST) Changes

Land Surface Temperature (LST) analysis was conducted to examine spatial and temporal thermal changes in the Kurunegala Municipal Council area between 1995 and 2024, and to understand how these changes are influenced by vegetation loss (NDVI) and built-up expansion (NDBI). The results indicate a consistent increase in surface temperature over the study period, with mean LST rising from 24.6C^{o} (1995) to 28.6C^{o} (2024) and maximum values reaching 34.1C^{o} in 2024, indicating a clear intensification of surface heating.

Spatially, the highest LST values are concentrated in Kurunegala Town–Central, Kurunegala Town–Bazaar, Kurunegala Town–North, and Malkaduwawa GN divisions, where dense commercial development, transport infrastructure, and administrative functions dominate the land surface. These areas exhibit strong positive NDBI values and very low NDVI values, indicating extensive built-up surfaces with minimal vegetation cover. This combination of high NDBI and low NDVI results in maximum heat absorption, reduced evapotranspiration, and continuous surface warming, contributing significantly to the Urban Heat Island (UHI) effect. Similar patterns have been widely reported in urban climate studies, where impervious surface expansion strongly increases LST through reduced latent heat flux and increased sensible heat storage (Weng, 2001; Li et al., 2012).

In contrast, moderate LST values are observed in transitional GN divisions such as Gettuwana, Theliyagonna, Henamulla, and Iluppugedara, where mixed land use patterns exist with fragmented vegetation and expanding built-up areas, resulting in intermediate NDVI and gradually increasing NDBI values. This reflects an ongoing land transformation stage where vegetation loss and urban expansion occur simultaneously, creating spatial thermal heterogeneity.

Relatively lower LST values are recorded in more vegetated and peri-urban GN divisions such as Ethiniwetunugala, Heraliyawala, and areas surrounding Kurunegala Lake, where higher NDVI and lower NDBI values promote cooling through evapotranspiration and shading effects. These vegetated zones act as local thermal buffers, reducing surrounding surface temperatures. Such cooling effects of vegetation and water bodies are well documented in remote sensing-based urban thermal studies, where NDVI is consistently negatively correlated with LST (Zha et al., 2003; Voogt & Oke, 2003).

The integrated NDVI–NDBI–LST relationship clearly demonstrates a strong biophysical interaction controlling thermal patterns in the study area. A clear inverse relationship exists between NDVI and LST, where areas experiencing vegetation loss show increasing surface temperatures. This is consistent with findings from Seto et al. (2012), who reported that rapid urban expansion leads to fragmentation and reduction of vegetated land, intensifying urban thermal environments. Conversely, a strong positive relationship is observed between NDBI and LST, as built-up areas expanded from 2.91 km² to 5.738

km², increasing impervious surfaces that enhance heat retention and reduce moisture availability (Rimal et al., 2018; Dewan & Yamaguchi, 2009).

Although LST shows an overall increasing trend, minor fluctuations in minimum temperature values (23.6 C° in 2015 to 23.2 C° in 2024) can be attributed to localized cooling effects from remaining vegetation patches and water bodies, particularly around Ethugala and Kurunegala Lake, as well as seasonal variations in satellite image acquisition. Such microclimatic buffering effects are commonly observed in heterogeneous urban landscapes where fragmented green spaces still influence local thermal conditions (Weng, 2001).

Overall, the results confirm that thermal variation in the Kurunegala Municipal Council area is not random but systematically controlled by land cover transformation, where urban GN divisions (high NDBI, low NDVI) exhibit high LST, vegetated GN divisions (high NDVI, low NDBI) exhibit low LST, and transitional GN divisions show moderate thermal conditions. This demonstrates a clear coupled environmental system where increasing urbanization drives vegetation loss and surface warming, consistent with established urban climate literature (Weng, 2001; Zha et al., 2003; Rimal et al., 2018).

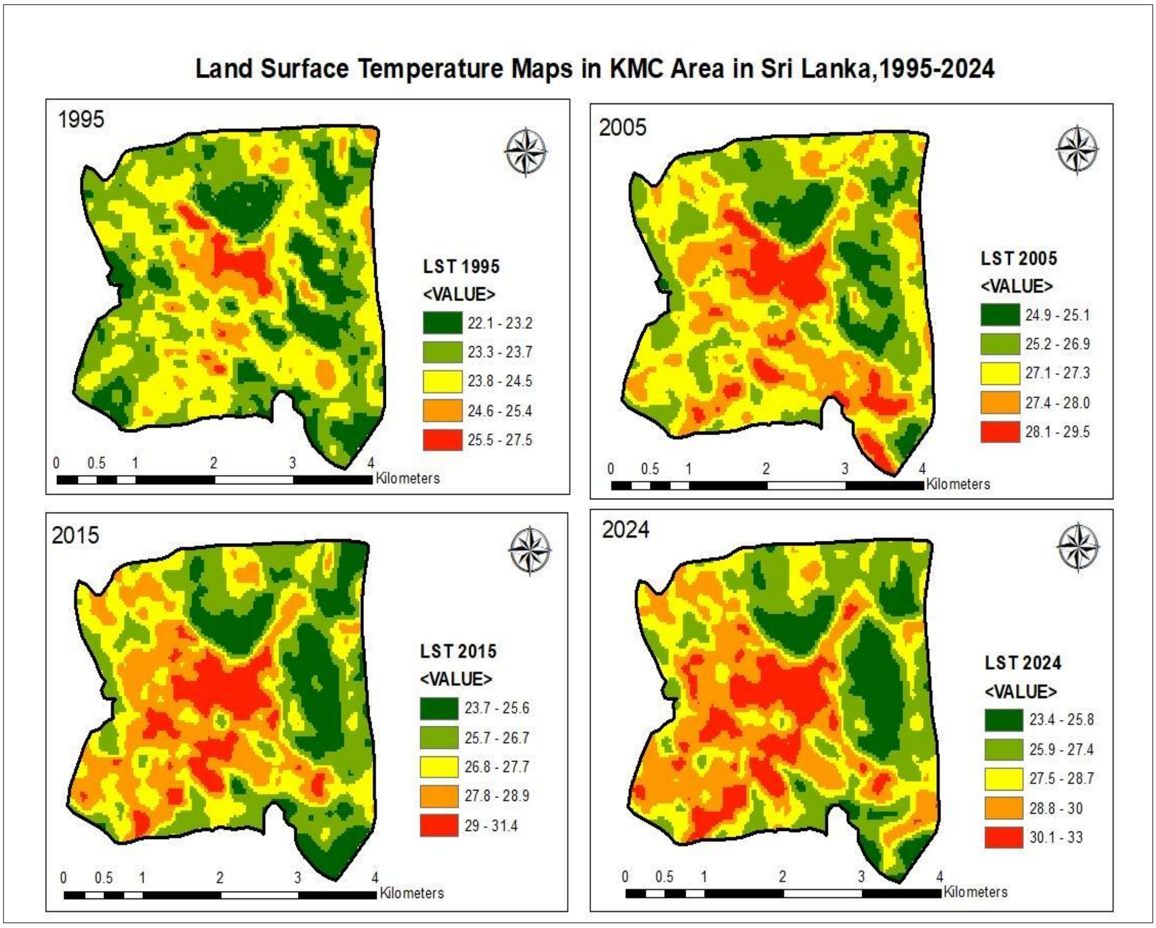

Figure 6: Land Surface Temperature (LST) Map, Kurunegala Municipal Council (KMC) Area, 1995-2024

Source: Created by the author using Landsat data (1995–2024) from USGS Earth Explorer and the 1:50000 topographic map from the Survey Department of Sri Lanka, 2025.

Table 5: Descriptive Statistics of Land Surface Temperature (LST)1995-2024

Year	1995	2005	2015	2024
Maximum temperature (C^0)	27.4	9.5	31.3	34.1
Minimum temperature (C^0)	22.1	24.9	23.6	23.2
Mean temperature (C^0)	24.6	26.8	27.4	28.6
Standard Deviation (C^0)	1.18	1.21	1.53	1.88

Source: Created by the author based on the Land Surface Temperature, 2025

Urban Heat Island Dynamics

The Urban Heat Island (UHI) dynamics were analysed to evaluate the thermal contrast between urban and non-urban surfaces within the Kurunegala Municipal Council (KMC) area from 1995 to 2024. The results indicate that UHI intensity does not follow a strictly linear increasing trend, even though Land Surface Temperature (LST) shows an overall upward pattern. This apparent fluctuation is largely attributed to variations in vegetation cover, seasonal atmospheric conditions during image acquisition, and spatial heterogeneity in urban expansion, which influence surface energy balance and heat redistribution processes.

Figure 8 illustrates the spatial distribution of UHI intensity across the study period. In 1995, UHI values ranged from 8.27C^{o} to 13.63C^{o}, indicating moderate thermal contrast between built-up and surrounding vegetated areas. By 2005, UHI intensity increased significantly, reaching a maximum of 19.38C^{o}, corresponding to rapid urban expansion and increasing impervious surface coverage in the urban core and along major transport corridors. In 2015, a temporary reduction in UHI intensity was observed (maximum 11.81C^{o}), which can be linked to relatively higher vegetation presence and localized cooling effects in peri-urban zones and around water bodies, particularly near the Kurunegala Lake and surrounding green patches. However, despite this reduction, persistent heat concentration remained evident in the city center and commercial zones. By 2024, UHI intensity increased again, with values ranging from 7.40C^{o} to 17.01C^{o}, reflecting intensified built-up expansion, densification of commercial areas, and reduction of vegetated land.

Spatially, the UHI pattern consistently shows a strong thermal core in the urban center, expanding outward along transport corridors where infrastructure development is concentrated, while comparatively lower UHI values are observed in vegetated areas and water bodies due to higher evapotranspiration and heat absorption capacity. This spatial structure demonstrates a clear relationship between vegetation loss, urban expansion, and increasing thermal stress, confirming that built-up growth is a major driver of UHI formation in the KMC area.

When compared with similar municipal-scale studies in South Asia and tropical urban environments, the observed UHI intensity falls within the moderate to high range reported in rapidly urbanizing cities, although the episodic fluctuations highlight the strong influence of local land cover and seasonal variability rather than purely long-term urban growth trends. These findings are consistent with studies that emphasize the role of vegetation fragmentation and impervious surface expansion in controlling urban thermal environments.

The implications of increasing UHI intensity are significant for urban sustainability and public health. Elevated surface temperatures can contribute to heat stress, reduced outdoor thermal comfort, increased energy demand for cooling, and heightened risk of heat-related illnesses, particularly in densely populated urban cores. Therefore, integrating urban greening strategies, preserving water bodies, and controlling unplanned built-up expansion are essential for mitigating future UHI impacts in the KMC area.

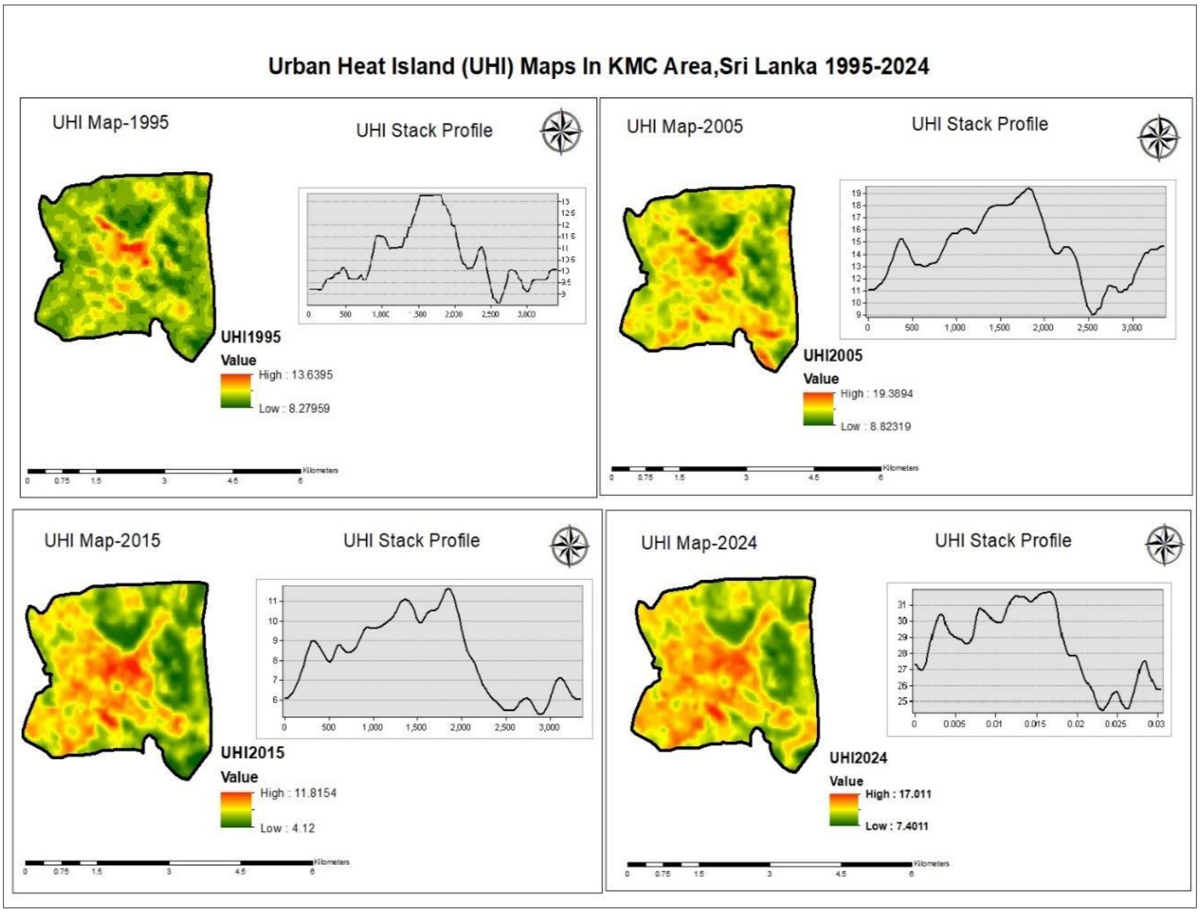

Figure 7: Urban Heat Island (UHI) Map, Kurunegala Municipal Council Area, 1995-2024

Source: Created by the author using Landsat data (1995–2024) from USGS Earth Explorer and the 1:50,000 topographic map from the Survey Department of Sri Lanka, 2025.

The Environmental Criticality Index (ECI)

The Environmental Criticality Index (ECI) analysis was conducted to assess the spatial and temporal variation of environmental sensitivity within the Kurunegala Municipal Council (KMC) area for the years 1995, 2005, 2015, and 2024 (Figure 8). The results indicate a long-term transition from predominantly non-critical environmental conditions toward more environmentally stressed categories, reflecting progressive land-use transformation associated with urban expansion. Such spatial transitions are commonly observed in rapidly urbanizing cities where land cover conversion increases environmental pressure (Li et al., 2012; Dewan & Yamaguchi, 2009).

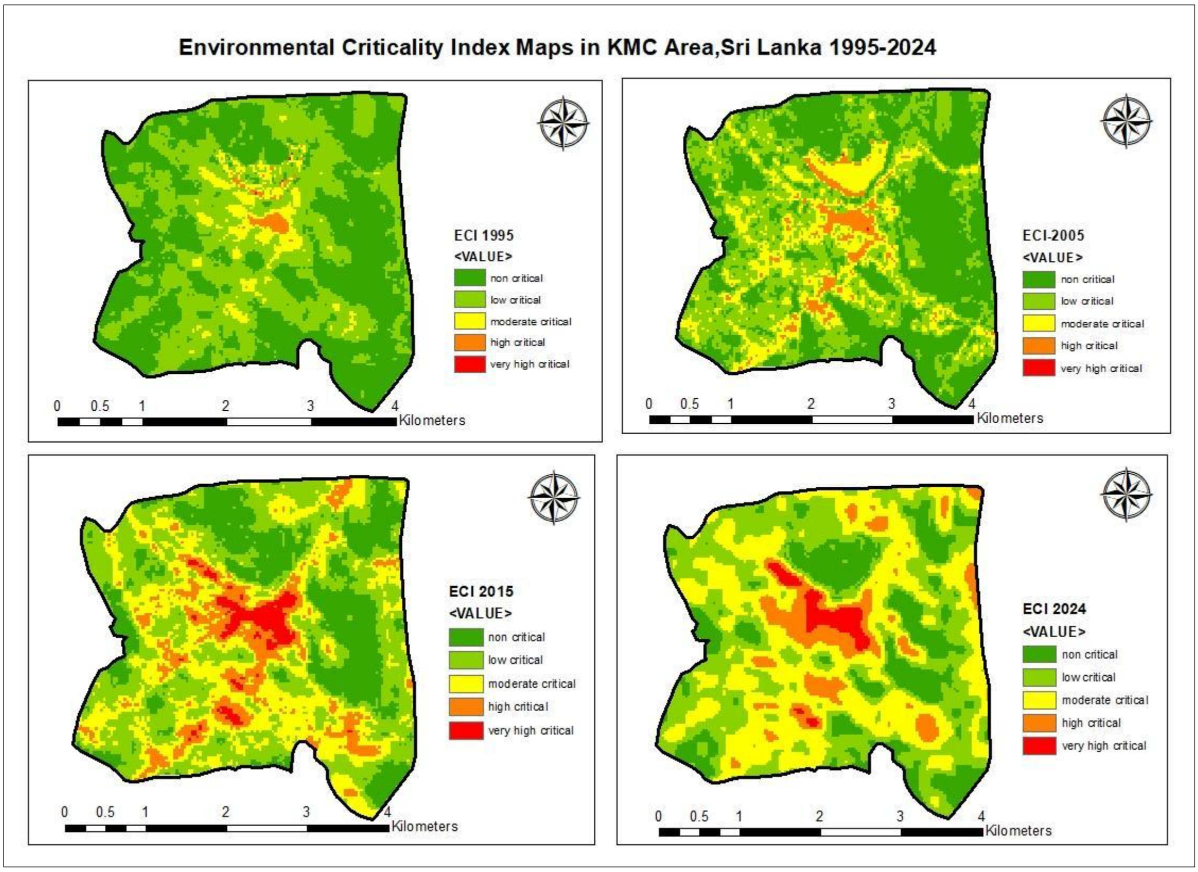

Figure 8: Environmental Criticality Map, Kurunegala Municipal Council Area, 1995-2024

Source: Created by the author using Landsat data (1995–2024) from USGS Earth Explorer and the 1:50,000 topographic map from the Survey Department of Sri Lanka, 2025.

In 1995, non-critical zones dominated the landscape (51.42%), particularly in peripheral GN divisions such as Siyambalapitiya, Yanthampalawa outskirts, and more vegetated sections of Hidyala and Gangoda GN areas, where vegetation cover remained relatively intact. By 2024, these non-critical areas had reduced to 18.07%, mainly confined to fragmented peri-urban patches and remaining vegetated pockets in outer GN divisions such as Bamunugedara fringe areas and parts of Gettuwana buffer zones. Similar declines in low-stress ecological zones have been widely documented in urban growth studies using remote sensing, where expansion typically occurs outward from urban cores into vegetated land (Seto et al., 2012).

Moderate critical areas show a strong and continuous expansion from 5.54% in 1995 to 36.64% in 2024. This expansion is mainly concentrated along rapidly urbanizing GN divisions such as Kurunegala town core GN divisions (including Central Kurunegala, Gettuwana urban fringe, and Kanda Wela areas), particularly around transport infrastructure such as the Kurunegala railway station and central bus terminal. These GN divisions have experienced increasing residential and commercial densification, which aligns with findings that transport accessibility strongly influences spatial urban expansion and environmental degradation (Herold et al., 2005).

High critical zones also increased from 0.95% in 1995 to 8.52% in 2024, particularly within densely built GN areas such as Pothuhera industrial influence zone, Kospotha commercial clusters, and sections of Wilgoda urban expansion corridor. These areas reflect increasing impervious surface cover, reduced ecological permeability, and intensified land-use conversion, which are commonly associated with elevated environmental stress in urban systems.

Very high critical areas, although still limited in spatial extent (2.74% in 2024), are mainly concentrated in highly congested GN divisions such as Kurunegala city center GN areas near the bus stand, railway station surroundings, and parts of Lake Round (Kurunegala Tank perimeter urbanized edge). These zones are characterized by minimal open space, high surface sealing, and strong anthropogenic pressure. Such conditions are typically associated with higher land surface temperatures and reduced vegetation cooling effects.

It is important to note that the observed spatial patterns are derived from remote sensing–based land surface characteristics. In future improvements, masking water bodies such as Kurunegala Tank and associated wetland buffers, as well as dense vegetation patches, is recommended prior to classification to improve ecological accuracy and reduce misclassification in stable natural zones.

Overall, the spatial distribution of ECI classes indicates a gradual outward expansion of moderate to high critical zones from the urban core GN divisions toward peri-urban GN divisions such as Gettuwana, Bamunugedara, and Wilgoda fringes, while non-critical zones become increasingly fragmented. This spatial restructuring is consistent with global urbanization trends where environmental degradation intensifies along urban expansion gradients.

The relationship between vegetation cover and surface temperature further supports these patterns. NDVI–LST regression results indicate a consistent negative relationship across all years, confirming the cooling role of vegetation. However, the strength of this relationship varies over time, suggesting that increasing impervious surfaces within central GN divisions have weakened the moderating influence of vegetation on surface temperature.

Overall, the ECI results should be interpreted as spatial indicators of environmental stress derived from land surface characteristics rather than direct measures of governance or policy effectiveness. The observed trends primarily reflect land-use change dynamics and biophysical responses to urban expansion within specific GN divisions of the Kurunegala Municipal Council area.

Table 7: Area covered by the Environmental Critical Map (km), Kurunegala Municipal Council Area, 1995-2024

ECI Classes	1995		2005		2015		2024	
	km	%	km	%	km	%	km	%
Non critical	6.05	51.42	5.17	43.86	2.62	22.23	2.13	18.07
Low critical	4.95	42.05	4.31	36.59	4.32	36.72	4.02	34.14
Moderate critical	0.653	5.54	1.85	15.75	3.223	27.35	4.32	36.64
High critical	0.113	0.95	0.44	3.78	1.282	10.88	1.00	8.52
Very high critical	0.002	0.03	0.003	0.02	0.289	2.45	0.327	2.74

Source: Created by the author based on the ECI, 2025

Relationship between Remote Sensing Indices

NDVI and LST

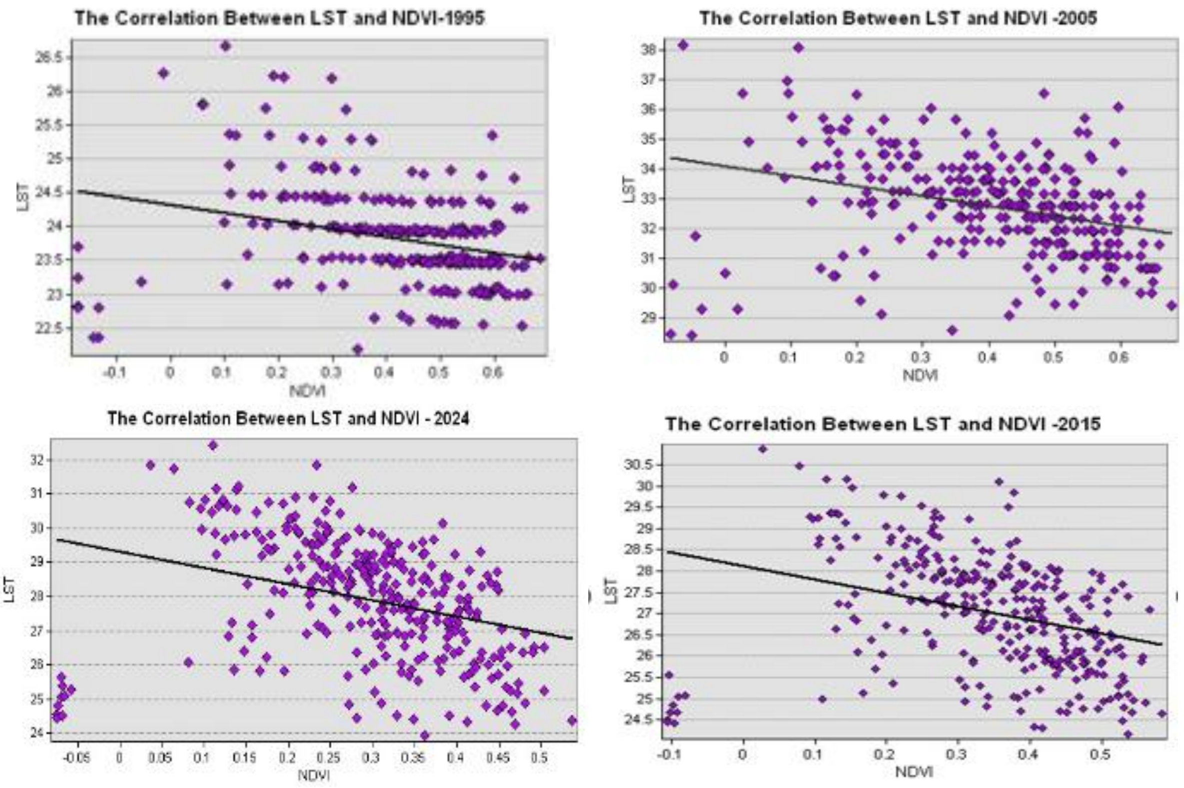

Figure 9: Correlation between LST and NDVI 1995-2024

Source: Created by the author, 2025

Table 8: Numerical correlation between LST and NDVI, 1995-2024

Year	Y value	Observation coefficient (R^2)	P value	Correlation value	Correlation level
1995	-1.1835x + 24.3107	0.079 (7.9%)	5.76E-07	-0.281	Negative
2005	-3.3465x + 34.1157	0.103 (10.3%)	8.48E-09	-0.321	Moderate negative
2015	-3.1668x + 28.1076	0.103 (10.2%)	9.33E-09	-0.321	Moderate negative
2024	-4.7429x + 29.3281	0.101 (10.1%)	1.28E-08	-0.317	Moderate negative

Source: Created by the author, 2025

In 1995, the regression analysis also revealed a negative correlation between NDVI and LST. With a correlation coefficient of -0.281 and an R^2 value of 0.079, only 7.9% of the variation in LST could be explained by changes in vegetation cover (Table 4). The regression equation for this year was LST = -1.1835x + 24.3107, indicating a negative relationship between NDVI and LST. In the early stages of urban growth, vegetation still played a cooling role.

By 2005 (Table 8), the correlation coefficient between NDVI and LST had increased to 0.321. This is a moderate negative correlation. The R^2 value also increased to 0.103 or 10.3%. This suggests that vegetation changes are starting to have a greater impact on surface temperatures. The regression equation LST = -3.3465x + 34.1157 shows a negative slope, indicating that temperatures have increased with vegetation loss, compared to the previous one.

In 2015, the correlation coefficient was 0.321, and the R^2 value dropped slightly to 0.102. The regression model LST = -3.1668x + 28.1076 still showed a moderate negative correlation. This reinforces the idea that vegetation loss is a more direct contributor to rising LST. This transformation not only reduced the cooling effect of vegetation but also increased surface heating. In 2024, the correlation was moderately positive at 0.317, and the R^2 value was 0.101. The regression equation LST = -4.7429x + 29.3281 showed that the effect of vegetation loss on LST was even more pronounced. Although the explanatory power of NDVI in predicting LST changes has not increased significantly, the slope of the regression line suggests that each unit of vegetation loss now corresponds to a greater increase in surface temperature than in previous years.

While the R^2 values remain moderate (7.9% to 10.3%), they consistently indicate a statistically significant relationship between vegetation loss and LST increase.

The regression analysis in 1995 also reveals a negative correlation between NDVI and LST. In the early stages of urban growth, vegetation still played a cooling role. By 2005, vegetation changes had begun to have a greater impact on surface temperatures. Temperatures have increased with vegetation loss than before, when the regression equation showed a negative slope. The year 2015, with its moderate negative correlation, reinforces the idea that vegetation loss is contributing more directly to rising LST. This transformation not only reduced the cooling effect of vegetation but also increased surface warming. Although the explanatory power of NDVI in predicting LST changes in 2024 has not increased significantly, the slope of the regression line suggests that each unit of vegetation loss now corresponds to a greater increase in surface temperature than in previous years. (Figure 9)

LST and NDBI

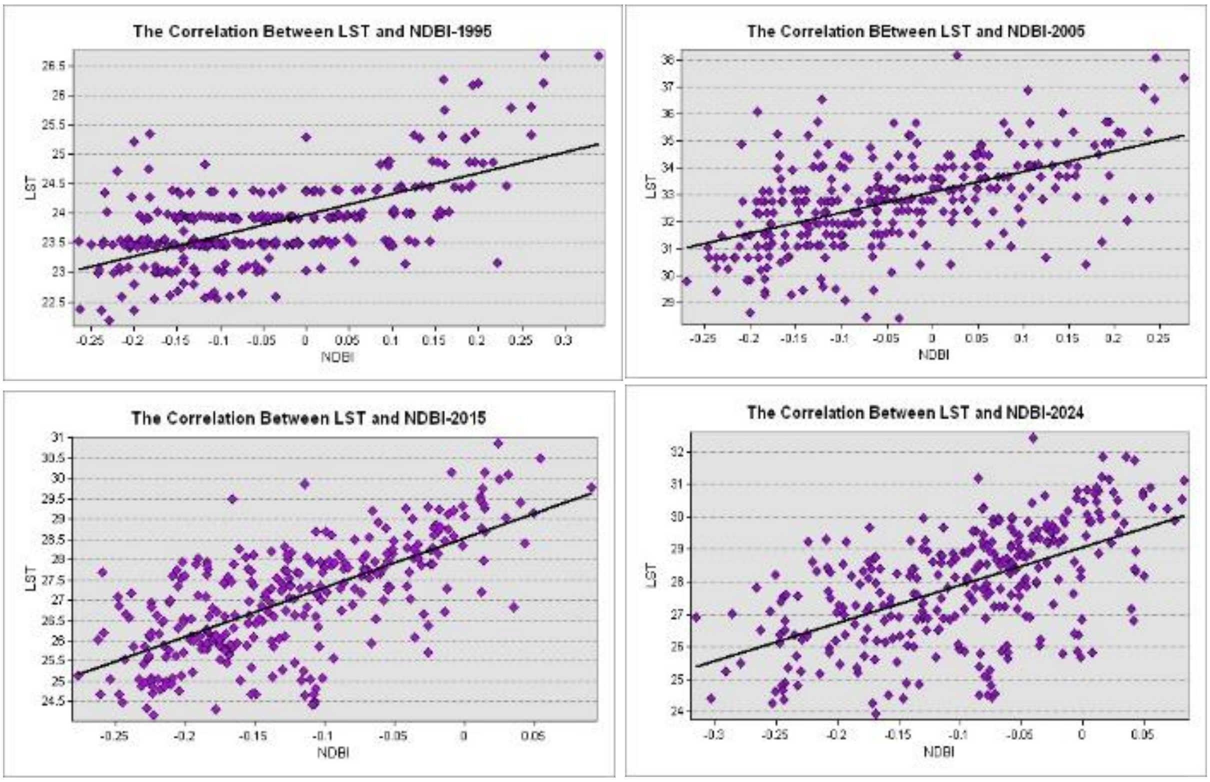

Figure 10: Correlation between LST and NDBI 1995-2024

Source: Created by the author, 2025

Table 9: Numerical correlation of LST and NDBI correlation, 1995-2024

year	Y value	Observation coefficient (R^2)	P value	Correlation value(r)	Correlation level
1995	Y = 2.8546X + 21.745	0.215	0.000	0.463	Moderate positive
2005	Y = 3.2944X + 24.890	0.2205	0.000	0.470	Moderate positive
2015	Y = 5.1087X + 28.008	0.1833	0.000	0.428	Moderate positive
2024	Y = 9.7284X + 30.114	0.4750	0.000	0.689	Strong positive

Source: Created by the author based on LST and NDBI correlation, 2025

In 1995, the regression equation was LST = 2.8546X + 21.745 and the R^2 was 0.215, indicating that 21.5% of the variation in land surface temperature could be explained by changes in built-up area. The correlation coefficient was 0.463, indicating a moderate positive correlation between built-up area and LST. It is clear that LST tended to increase accordingly as built-up area increased. Although Kurunegala was still in its early stages of urban growth, the statistical results already show a clear relationship between human-induced land cover changes and thermal behavior.

In 2005, the relationship between built-up area and LST remained relatively stable. The regression model for this year was LST = 3.2944X + 24.890, and the R^2 value increased slightly to 0.2205. This means that 22.05% of the variation in LST can be attributed to built-up area changes. The correlation coefficient increased slightly to 0.470, which still indicates a moderate positive correlation. This stage represents a transitional period when land cover change due to construction and infrastructure development began to contribute significantly to local temperature increases.

In 2015, the regression equation was LST = 5.1087X + 28.008. LST increased much faster in response to each unit increase in built-up area. The R^2 dropped to 0.1833. This means that only 18.33% of the variation in LST can be explained by changes in built-up areas. The correlation coefficient remained in the moderate range of 0.428. The decline in R^2 also highlights that urbanization continues to contribute to rising surface temperatures due to the increased complexity of urban land use. By 2024, the regression model had changed significantly to LST = 9.7284X + 30.114, with the highest R^2 value among all years being 0.4750. This means that 47.5% of the variation in land surface temperature can now be explained by changes in built-up areas. This is more than double the value in 1995. The correlations increased sharply to R^2 0.689, indicating a strong positive correlation. This significant increase in both slope and R^2 indicates that the relationship between urbanization and LST has intensified. The increasing explanatory power of built-up areas suggests that urban land cover is the dominant driver of LST variations in the Kurunegala Municipal Council area.

NDBI and NDVI

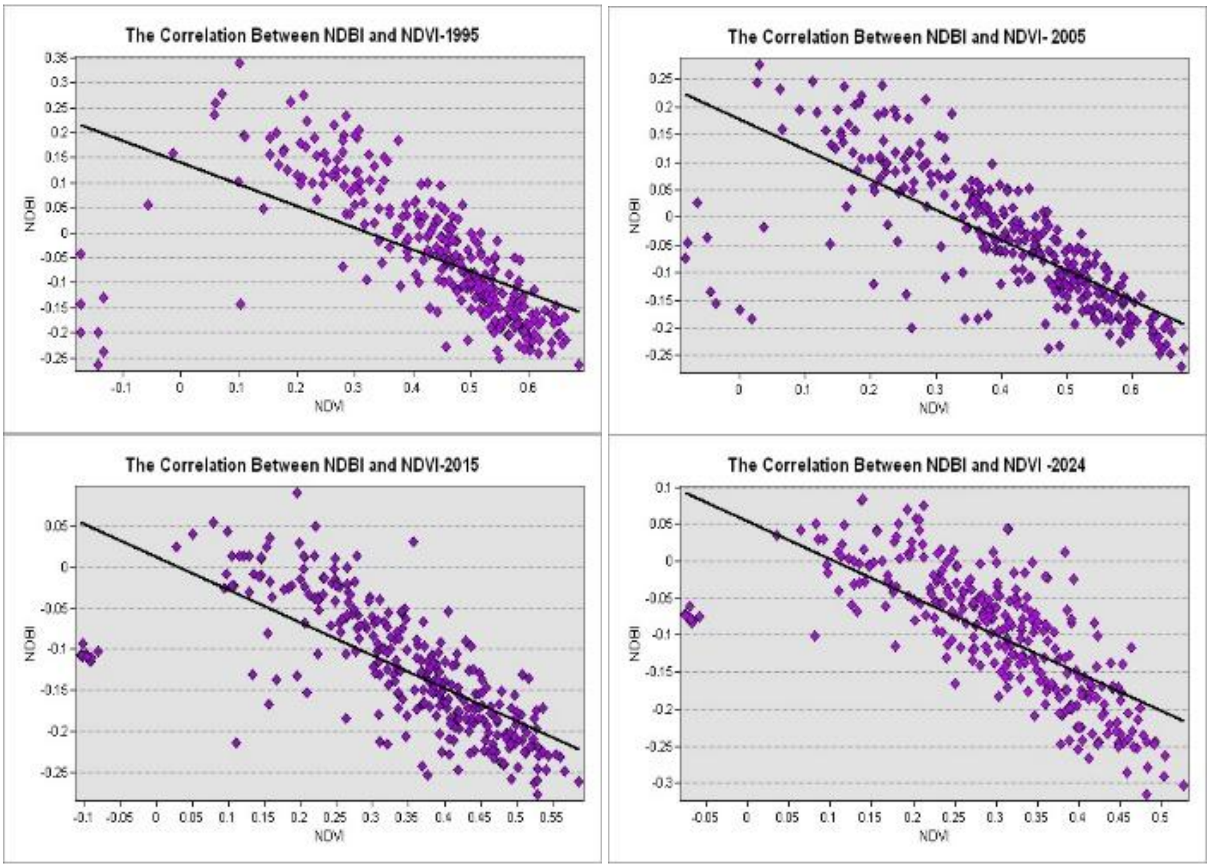

Figure 11: Correlation between NDBI and NDVI 1995-2024

Source: Created by the author, 2025

Table 10: Numerical correlation between NDBI and NDVI 1995-2024

Year	Y value	Observation coefficient (R^2)	P value	Correlation value	Correlation level
1995	Y = -2.8546X + 34.745	0.215(19.8%)	0	-0.463	Moderate negative

2005	Y = 3.8944X + 24.890	0.2205(22.1%)	0	-0.470	Moderate negative
2015	Y = -5.1087X + 28.008	0.1833(18.3%)	0	-0.428	Moderate negative
2024	Y = 8.3592X + 30.014	0.4750(43.7%)	0	-0.689	Strong negative

Source: Created by the author based on the correlation between NDBI and NDVI, 2025

In 1995, the R^2 value was 0.215. This means that 19.8% of the variation in vegetation cover can be explained by changes in built-up area. The correlation coefficient (r) was -0.463, indicating a moderate negative correlation. This suggests that even in the early stages of urban growth in Kurunegala, there was a measurable impact on vegetation loss due to increased construction and land conversion. Although the correlation is not yet strong, it reflects a clear trend that vegetation land has started to decline as urbanization accelerates. By 2005, the R^2 had increased slightly to 0.2205 (22.1%). The R also showed a moderate negative correlation of -0.470. Pressure on green spaces has continued to grow as built-up areas continue to expand. Vegetation loss was becoming more predictable based on the extent of urban growth. Although the increase in R^2 was modest, it highlights a consistent trend that urban growth is increasingly responsible for the reduction of vegetated land.

In 2015, the R^2 value fell slightly to 0.1833 (18.3%) and the correlation coefficient remained moderately negative at -0.428. This decline in R^2 may indicate that additional factors such as informal land use, mixed development patterns or reforestation in small areas have reduced the predictability of vegetation loss based on urban expansion alone. The relationship is still statistically significant and built-up growth has contributed to the reduction of vegetated areas throughout Kurunegala.

By 2024, the R^2 value had risen sharply to 0.4750. The R2- was 0.689, indicating a strong negative correlation between the increase in built-up area and the decrease in vegetation cover. Almost half of the changes in vegetation cover can now be directly explained by the growth of urban areas.

The study area is facing the impact of increasing land surface temperature, decreasing vegetation cover, and increasing built-up areas due to the gradual urban growth. The environmental critical index has also increased by 2024 due to the increase in land surface temperature due to the decrease in vegetation cover. Accordingly, it is clear that the environmental impacts caused by urban growth discussed in this chapter are correlated with each other.

As a summary the relationship between NDVI and LST showed a negative correlation, indicating that areas with higher vegetation density generally experienced lower surface temperatures due to vegetation cooling effects. The relationship between NDBI and LST showed a positive correlation, demonstrating that expansion of built-up surfaces contributed to increased thermal conditions. The negative relationship between NDBI and NDVI confirms that urban expansion occurred through conversion of vegetated areas into impervious surfaces. Correlation coefficient (r), coefficient of determination (R^2), and p-values are presented in Annex Table X and indicate statistically significant relationships ($p < 0.05$).

Conclusion

The Kurunegala Municipal Council (KMC) area experienced significant urban growth between 1995 and 2024, driven by population increase, housing expansion, infrastructure development, and economic activities. This study assessed the environmental impacts of urban growth using remote sensing and GIS techniques through the analysis of Land Use/Land Cover (LULC), Normalized Difference Vegetation Index (NDVI), Normalized Difference Built-up Index (NDBI), Land Surface Temperature (LST), and the Environmental Criticality Index (ECI). The findings indicate that urban expansion has substantially transformed the environmental landscape of the KMC area. Population growth and increased housing development accelerated the demand for land, resulting in the conversion of vegetation and other natural land covers into urban land uses. During the study period, vegetation cover declined from approximately 55.56% to 26.71%, reflecting a significant loss of urban green spaces and ecological resources. Simultaneously, built-up land increased from 2.91 km^2 to 5.738 km^2, demonstrating the continuous expansion of urban infrastructure and impervious surfaces. These land-use changes altered the spatial structure of the city and reduced the ecological functions provided by vegetation. The thermal environment of the KMC area also changed considerably, as evidenced by increasing LST values. The maximum LST increased from 27.4C° in 1995 to 34.1C° in 2024, indicating a strengthening Urban Heat Island (UHI) effect associated with urban expansion and vegetation loss. Statistical analyses further confirmed the relationship between urban growth and environmental change, showing a negative relationship between NDVI and LST and a positive relationship between NDBI and LST, highlighting the role of built-up surface expansion in increasing land surface temperatures. The ECI analysis revealed a progressive increase in environmentally critical areas, particularly within the urban core and rapidly developing peripheral zones, demonstrating the cumulative impacts of vegetation degradation, built-up expansion, and thermal stress. Although the study successfully identified long-term environmental changes using remote sensing data, limitations include the use of multi-temporal satellite imagery with varying atmospheric conditions and the reliance on secondary demographic data. Future studies should incorporate higher-resolution satellite imagery, advanced urban growth modelling techniques, and climate-related indicators to improve prediction accuracy and environmental assessment. From a policy perspective, the findings emphasize the need for sustainable urban planning strategies, including the protection and restoration of urban green spaces, promotion of compact and vertical development, implementation of urban greening programmes, and integration of

GIS and remote sensing technologies into urban planning and environmental management to support sustainable urban development in Kurunegala and other rapidly growing cities in Sri Lanka.

Acknowledgements

To my mother and father, who have always been the greatest light in my life without any regrets at every beginning, and to my supervisor, D.L.N.P. Liyanage in the Department of Geography and Management, Faculty of Social Sciences and Languages, Sabaragamuwa University of Sri Lanka, who have always encouraged me by giving me advice with enthusiasm and love, this would not have been possible without your guidance and advice. In honour of your undying respect for me, who have always bestowed love, respect and self-confidence upon me, I dedicate this work from a deep place in my soul to everyone who has illuminated my life and believed in me.

References

Avdan, U., & Jovanovska, G. (2016). Algorithm for automated mapping of land surface temperature using LANDSAT 8 satellite data. *Journal of Sensors, 2016*, 1–8. https://doi.org/10.1155/2016/1480307

Chen, Y., Li, X., Zheng, Y., Guan, Y., & Liu, X. (2014). Estimating the relationship between urban forms and energy consumption. *Landscape and Urban Planning, 130*, 108–116. https://doi.org/10.1016/j.landurbplan.2014.06.013

Dewan, A. M., & Yamaguchi, Y. (2009). Land use and land cover change in Greater Dhaka, Bangladesh: Using remote sensing and GIS techniques. *Journal of Geographical Sciences, 19*(4), 405–420. https://doi.org/10.1007/s11442-009-0405-3

Dewan, A. M., & Yamaguchi, Y. (2009). Using remote sensing and GIS to detect and monitor land use and land cover change in the Dhaka Metropolitan of Bangladesh. Journal of Geographic Information System, 1(3), 129–136. https://doi.org/10.4236/jgis.2009.13012

Eastman, J. R. (2012). *IDRISI Selva Manual*. Clark Labs, Clark University.

Estoque, R. C., Murayama, Y., & Myint, S. W. (2017). Effects of landscape composition and pattern on land surface temperature: An urban heat island study in the megacities of Southeast Asia. Science of the Total Environment, 577, 349-359.

Fernando, D., Wijesinghe, R., & Wickramasinghe, W. (2018). Urbanization and its impact on water resources: A case study of Kurunegala City. Environmental Impact Review, 12(2), 21–30.

Geneletti, D. (2004). A GIS-based decision support system to identify nature conservation priorities in an alpine valley. *Land Use Policy, 21*(2), 149–160. https://doi.org/10.1016/j.landusepol.2003.09.005

Glaeser, E. L. (2011). Cities, productivity, and quality of life. Science, 333(6042), 592–594. https://doi.org/10.1126/science.1209264

Herold, M., Goldstein, N. C., & Clarke, K. C. (2005). The spatiotemporal form of urban growth: Measurement, analysis and modeling. Remote Sensing of Environment, 86(3), 286–302. https://doi.org/10.1016/j.rse.2003.08.008

Intergovernmental Panel on Climate Change. (2021). Climate change 2021: The physical science basis. Contribution of Working Group I to the Sixth Assessment Report of the Intergovernmental Panel on Climate Change. Cambridge University Press. https://doi.org/10.1017/9781009157896

Lambin, E. F., & Geist, H. J. (Eds.). (2006). Land-use and land-cover change: Local processes and global impacts. Springer. https://doi.org/10.1007/3-540-32202-7

Li, X., Zhou, W., & Ouyang, Z. (2012). Forty years of urban expansion in Beijing: What is the relative importance of physical, socioeconomic, and neighborhood factors? Applied Geography, 38, 1–10. https://doi.org/10.1016/j.apgeog.2012.01.003

Li, X., Zhou, Y., & Asrar, G. R. (2012). A numerical investigation of the anthropogenic heat effect within urban areas. Environmental Research Letters, 7(3), 034003. https://doi.org/10.1088/1748-9326/7/3/034003

lysis. Sri Lanka Journal of Geography, 15(1), 34–50.

Malczewski, J. (2006). GIS-based multicriteria decision analysis: A survey of the literature. *International Journal of Geographical Information Science, 20*(7), 703–726. https://doi.org/10.1080/13658810600661508

Oke, T. R. (1982). The energetic basis of the urban heat island. *Quarterly Journal of the Royal Meteorological Society, 108*(455), 1–24. https://doi.org/10.1002/qj.49710845502

Perera, M. (2016). Urbanization and housing demand in Sri Lanka: A case study of Kurunegala. Journal of Urban and Regional Planning, 10(4), 78–92.

Perera, R., & Jayawardena, D. (2019). Remote sensing analysis of water body shrinkage in urban Sri Lanka: A case study of Kurunegala. Remote Sensing Applications, 7(3), 102–115.

Rajapaksha, S., & Perera, S. (2019). Land use change in the Kurunegala Urban Council area: A GIS and remote sensing anahttps://doi.org/10.1080/01431160010020106

Ranagalage M. Estoque R.C. Handayani H.H, Zhang X. Morimoto T. Tadono T. et al (2018b). Relation between urban volume and land surface temperature: a comparative study of planned and traditional cities in Japan. Sustainability10, 2366. 10.3390/su10072366

Rimal, B., Zhang, L., Keshtkar, H., & Rijal, S. (2018). Urban expansion and land use change detection using remote sensing and GIS in South Asian cities. Remote Sensing, 10(9), 1433. https://doi.org/10.3390/rs10091433

Rizwan, A. M., Dennis, L. Y. C., & Liu, C. (2008). A review on the generation, determination and mitigation of urban heat island. *Journal of Environmental Sciences*, *20*(1), 120–128. https://doi.org/10.1016/S1001-0742(08)60019-4

Rosenzweig, C., Solecki, W. D., Romero-Lankao, P., Mehrotra, S., Dhakal, S., & Ibrahim, S. A. (Eds.). (2018). Climate change and cities: Second assessment report of the Urban Climate Change Research Network. Cambridge University Press. https://doi.org/10.1017/9781316563878

SaputraL. I. A.JumadiA.SariD. N. (2023). Analysis of environmental criticality index (ECI) and distribution of slums in yogyakarta and surrounding areas using multitemporal landsat imagery. *Proc. Int. Conf. Geogr. Disaster Manag.*, 407–420. 10.2991/978-2-38476-066-4_26

Seto, K. C., Güneralp, B., & Hutyra, L. R. (2012). Global forecasts of urban expansion to 2030 and direct impacts on biodiversity and carbon pools. Proceedings of the National Academy of Sciences, 109(40), 16083–16088. https://doi.org/10.1073/pnas.1211658109

Sobrino, J. A., Jiménez-Muñoz, J. C., & Paolini, L. (2004). Land surface temperature retrieval from LANDSAT TM 5. *Remote Sensing of Environment*, *90*(4), 434–440. https://doi.org/10.1016/j.rse.2004.02.003

Sri Lanka Urban Development Authority. (2022). Urban expansion and environmental impact in Kurunegala. https://www.uda.gov.lk/

UN-Habitat. (2020). World cities report 2020: The value of sustainable urbanization. United Nations Human Settlements Programme. https://unhabitat.org/world-cities-report-2020-the-value-of-sustainable-urbanization

United Nations. (2018). World urbanization prospects: The 2018 revision. United Nations Department of Economic and Social Affairs. https://population.un.org/wup/Publications/

Voogt, J. A., & Oke, T. R. (2003). Thermal remote sensing of urban climates. Remote Sensing of Environment, 86 (3), 370–384. https://doi.org/10.1016/S0034-4257(03)00079-8

Voogt, J. A., & Oke, T. R. (2003). Thermal remote sensing of urban climates. *Remote Sensing of Environment*, *86*(3), 370–384. https://doi.org/10.1016/S0034-4257(03)00079-8

Weng, Q. (2001). A remote sensing–GIS evaluation of urban expansion and its impact on surface temperature in the Zhujiang Delta, China. *International Journal of Remote Sensing*, 22 (10), 1999–2014.

Weng, Q., Lu, D., & Schubring, J. (2004). Estimation of land surface temperature–vegetation abundance relationship for urban heat island studies. *Remote Sensing of Environment, 89*(4), 467–483. https://doi.org/10.1016/j.rse.2003.11.005

Xu, H. (2008). A new index for delineating built-up land features in satellite imagery. *International Journal of Remote Sensing*, *29*(14), 4269–4276. https://doi.org/10.1080/01431160802039957

Zha, Y., Gao, J., & Ni, S. (2003). Use of normalized difference built-up index in automatically mapping urban areas from TM imagery. *International Journal of Remote Sensing*, 24 (3), 583–594. https://doi.org/10.1080/01431160304987

Zha, Y., Gao, J., & Ni, S. (2003). Use of normalized difference built-up index in automatically mapping urban areas from TM imagery. *International Journal of Remote Sensing*, *24*(3), 583–594. https://doi.org/10.1080/01431160304987

Appendix

Correlation between LST and NDVI-1995

SUMMARY OUTPUT-1995

Regression Statistics	
Multiple R	0.281152332
R Square	0.079046634
Adjusted R Square	0.076017182
Standard Error	0.692093554
Observations	306

ANOVA					
	df	*SS*	*MS*	*F*	*Significance F*
Regression	1	12.49824214	12.49824	26.09272	5.76E-07
Residual	304	145.6140203	0.478993		
Total	305	158.1122624			

SUMMARY OUTPUT-2005

Regression Statistics	
Multiple R	0.321225595
R Square	0.103185883
Adjusted R Square	0.100245509
Standard Error	1.594218054
Observations	307

ANOVA					
	df	*SS*	*MS*	*F*	*Significance F*
Regression	1	89.1893779	89.18938	35.09277	8.48E-09
Residual	305	775.1670171	2.541531		
Total	306	864.356395			

SUMMARY OUTPUT-2015

Regression Statistics	
Multiple R	0.318004837
R Square	0.101127076
Adjusted R Square	0.098170258
Standard Error	1.66124831
Observations	306

ANOVA					
	df	*SS*	*MS*	*F*	*Significance F*
Regression	1	59.6079692	59.60797	34.884	9.33E-09
Residual	305	521.1682469	1.708748		
Total	306	580.7762161			

SUMMARY OUTPUT-2024

Regression Statistics	
Multiple R	0.320366983
R Square	0.102635004
Adjusted R Square	0.099692824
Standard Error	1.307191015
Observations	307

ANOVA					
	df	*SS*	*MS*	*F*	*Significance F*
Regression	1	94.38692575	94.38693	34.20131	1.28E-08
Residual	304	838.9627677	2.759746		
Total	305	933.3496935			

Correlation between NDVI and NDBI

SUMMARY OUTPUT-1995

Regression Statistics	
Multiple R	0.584256882
R Square	0.341356104
Adjusted R Square	0.339189512
Standard Error	0.103680527
Observations	306

ANOVA					
	df	*SS*	*MS*	*F*	*Significance F*
Regression	1	1.693655104	1.693655	157.5544	2.12E-29
Residual	304	3.267894099	0.01075		
Total	305	4.961549203			

SUMMARY OUTPUT-2005

Regression Statistics	
Multiple R	0.735579977
R Square	0.541077903
Adjusted R Square	0.539568291
Standard Error	0.081614632
Observations	306

ANOVA					
	df	*SS*	*MS*	*F*	*Significance F*
Regression	1	2.387429011	2.387429	358.4218	2.38E-53
Residual	304	2.024928245	0.006661		
Total	305	4.412357256			

SUMMARY OUTPUT-2015

Regression Statistics	
Multiple R	0.714180778
R Square	0.510054184
Adjusted R Square	0.50844252
Standard Error	0.054692731
Observations	306

ANOVA

	df	*SS*	*MS*	*F*	*Significance F*
Regression	1	0.946675333	0.946675	316.4768	5.10E-49
Residual	304	0.909353621	0.002991		
Total	305	1.856028953			

SUMMARY OUTPUT-2024

Regression Statistics	
Multiple R	0.710379354
R Square	0.504638826
Adjusted R Square	0.503009348
Standard Error	0.060214739
Observations	306

ANOVA

	df	*SS*	*MS*	*F*	*Significance F*
Regression	1	1.122891771	1.122892	309.6936	2.73E-48
Residual	304	1.102247701	0.003626		
Total	305	2.225139472			

Correlation between LST and NDBI

SUMMARY OUTPUT-1995

Regression Statistics	
Multiple R	0.55441645
R Square	0.307377601
Adjusted R Square	0.305099237
Standard Error	1.402998441
Observations	306

ANOVA

	df	*SS*	*MS*	*F*	*Significance F*
Regression	1	62.76305873	62.76306	191.1576	4.57E-34
Residual	304	99.81276844	0.328331		
Total	305	162.5758272			

SUMMARY OUTPUT-2005

Regression Statistics	
Multiple R	0.62133249
R Square	0.386054064
Adjusted R Square	0.384034505
Standard Error	0.57300216
Observations	306

ANOVA

	df	*SS*	*MS*	*F*	*Significance F*
Regression	1	265.5606018	265.5606	134.9116	4.66E-26
Residual	304	598.3950063	1.968405		
Total	305	863.9556081			

SUMMARY OUTPUT-2015

Regression Statistics	
Multiple R	0.68578221
R Square	0.470297239
Adjusted R Square	0.468554796
Standard Error	1.00398284
Observations	306

ANOVA					
	df	*SS*	*MS*	*F*	*Significance F*
Regression	1	272.0610421	272.061	269.9068	7.50E-44
Residual	304	306.4263894	1.007982		
Total	305	578.4874315			

SUMMARY OUTPUT-2024

Regression Statistics	
Multiple R	0.569118439
R Square	0.323895797
Adjusted R Square	0.32167177
Standard Error	1.444527773
Observations	306

ANOVA					
	df	*SS*	*MS*	*F*	*Significance F*
Regression	1	303.8904505	303.8905	145.6348	1.16E-27
Residual	304	634.3447881	2.08666		
Total	305	938.2352385			